

Article

The Effect of Thermal and Moisture Stress on Insulation Deterioration Law of Ionic Contaminated High-Voltage Printed Circuit Board of Electronic Power Conditioner

Cong Hu^{1,2,*}, Wei Zheng^{1,2}, Bin Zhao¹, Yu Fan¹, Hong Li¹, Kun Zheng³  and Gang Wang^{1,*}¹ Aerospace Information Research Institute, Chinese Academy of Sciences, Beijing 100094, China² School of Electronic, Electrical and Communication Engineering, University of Chinese Academy of Sciences, Beijing 100049, China³ Key Laboratory of Science and Technology on High-Tech Polymer Materials, Chinese Academy of Sciences, Beijing 100190, China

* Correspondence: hucong@aircas.ac.cn (C.H.); wanggang002412@aircas.ac.cn (G.W.); Tel.: +86-135-8168-5224 (C.H.)

Abstract: Since the electronic power conditioner (EPC) is a crucial part applied of a Space Travelling-wave Tube Amplifier (STWTA), the reliability issue must be considered. Of all the failure modes of an EPC, the insulation failure of an EPC in thermal and moist environments is the most serious, and needs special attention. By investigating the influence of contamination, humidity, and temperature on surface insulation resistance (SIR) and surface discharge, we focused on the determination of the insulation failure boundary in an EPC. Considering real working conditions, we used the typical circuit applied in the EPC as the test object. The insulation deterioration phenomenon under different thermal and moisture stress was studied. The results show that: (1) SIR of the samples did not change with contamination levels when the relative humidity (RH) was below 70%. When RH was higher than 75%, the SIR began to vary with temperature and ionic contaminant concentration. (2) Even if the samples were not contaminated (the ionic contamination concentration was less than 1.56 $\mu\text{g}/\text{cm}^2$), the deterioration of the SIR still occurred at 85 °C/90% RH. (3) The insulation failure boundary caused by surface discharge, and the degree of electrical erosion were related to humidity, pollution, voltage and temperature. To improve the failure caused by insulation, encapsulation was used. Experiments showed that encapsulation is an effective protection method to prevent insulation deterioration.

Keywords: Space Travelling-Wave Tube Amplifier (STWTA); electronic power conditioner (EPC); surface insulation resistance (SIR); surface discharge; ionic contaminant; encapsulation



Citation: Hu, C.; Zheng, W.; Zhao, B.; Fan, Y.; Li, H.; Zheng, K.; Wang, G. The Effect of Thermal and Moisture Stress on Insulation Deterioration Law of Ionic Contaminated High-Voltage Printed Circuit Board of Electronic Power Conditioner. *Energies* **2022**, *15*, 9616. <https://doi.org/10.3390/en15249616>

Academic Editor: Pawel Rozga

Received: 15 November 2022

Accepted: 15 December 2022

Published: 18 December 2022

Publisher's Note: MDPI stays neutral with regard to jurisdictional claims in published maps and institutional affiliations.



Copyright: © 2022 by the authors. Licensee MDPI, Basel, Switzerland. This article is an open access article distributed under the terms and conditions of the Creative Commons Attribution (CC BY) license (<https://creativecommons.org/licenses/by/4.0/>).

1. Introduction

The space traveling-wave tube amplifier (STWTA) is a key component of a satellite system for satellite communication and the spaceborne transponder. It is mainly responsible for the amplification, forwarding, and transmission of microwave signals [1]. As a critical component of STWTA [2], the electronic power conditioner (EPC) is required to undergo several months of environmental simulation tests during the development process [3]. It often happens that the sampling value of EPC increases in thermal and moisture stress environments, which leads to telemetry abnormality of the TWTA. The main reason for the increase in sampling value is leakage currents on the high-voltage printed circuit board (HV-PCB) surface due to a diminution in surface insulation resistance (SIR). Researchers believe that the presence of contamination of the HV-PCB surface acts as a factor in surface insulation resistance deterioration [4].

Contamination of the PCB mainly originates from processes of PCB manufacture, handling, operating environment, storage, and transportation [4,5]. Commonly found contaminations are residual salts from electroplating, etching, and soldering, flux residues [6–8],

dust particles [9–11], and even fingerprints of sweat. Residues and contamination in the manufacturing process, and improper operation cannot only affect SIR but also lead to electrochemical migration (ECM) [4,5], which is generally considered to be the failure mechanism most relevant to insulation failure behavior [12].

Research institutions such as Bell Labs (where ECM was first discovered), the Technical University of Denmark, the KTH Royal Institute of Technology, and the Beijing University of Posts and Telecommunications have conducted extensive research on the decrease in surface insulation resistance and aggravation in ECM caused by PCB surface contamination, as well as protection methods. Through the temperature-humidity-bias test [13–15], water drop test [16], thin electrolyte layer test [17], and electrochemical test on different types of PCB samples, different surface contaminants, and different protection methods, researchers have shown that: (1) under a certain humidity condition, the presence of contaminations will affect SIR and ECM [4,18]; (2) compared with non-cleaning flux residue containing weak organic acid active agents [7,19], ionic contaminations have a greater impact on the decrease of SIR [20], while the residue of moderately active rosin flux has little contribution to the degradation of SIR [21,22]; (3) soluble inorganic salts contained in natural dust in the air become one of the main reasons for the failure of the circuit board [9–11,23]; (4) the deterioration of SIR and ECM are closely related to humidity, temperature and applied voltage [24,25]; (5) PCBs are generally coated for protection [21,26], while integrated circuits are usually encapsulated to counter the effects of ECM [27].

It is worth noting that previous studies were all based on low-voltage circuits with small spacing between adjacent electrodes, operating voltage of only a few volts, and electric field strengths of only 100~1000 V/cm [28]. In addition, researchers usually used standard Y-type and comb circuits as experimental test circuits, test components are surface mount devices (SMD), while high-voltage applications were rarely reported. Compared with low-voltage circuits, the typical operating voltage of an EPC used in space is 4 kV~10 kV, and the electric field intensity is much higher than that of the low-voltage circuit [3]. HV-PCB welding of the EPC uses medium active rosin flux, and the pollution source that affects the insulation performance of the EPC is mainly ionic contamination. In high electric field strength, temperature, and humidity environments, surface contamination may cause two forms of insulation failure: surface insulation resistance (SIR) decline, and surface discharge [29]. Unfortunately, the effect of temperature, moisture, and ionic contamination on high-voltage insulation failure is rarely reported. Nevertheless, among all the failure modes of EPC, insulation failure in a temperature and humidity environment is the most serious one, and further affects the reliability of the EPC. As a result, in order to improve high-voltage insulation, it is necessary to investigate the effect of thermal and moisture stress on the insulation of ionic contamination of the high-voltage PCB of an EPC.

In this work, NaCl was used as the equivalent ionic contamination, and an EPC sampling equivalent circuit was used as the research object to study the insulation performance change of the EPC under the condition of temperature-humidity-bias. The sampling value of the divider resistance was used to characterize this change, which in actual products causes telemetry abnormality of TWTA. The influence of temperature, humidity, voltage, and surface ionic contamination on the insulation performance of the EPC was obtained. The temperature and humidity boundary conditions from the start point of failure to the occurrence of surface discharge were determined.

2. Materials and Methods

2.1. Experiment Design

A high-voltage sampling circuit is a common circuit form of EPC. The SIR of a PCB can be calculated by measuring the variation of sampling value of divider resistance in the sampling circuit. An EPC sampling equivalent circuit (Figure 1) was designed to quantify the concentration of ionic contaminants.

The test boards of HV-PCBs consisted of an FR-4 laminate with a thickness of 2 mm, which were consistent with the product. The size of the divider resistor area was

10 mm × 30 mm, and the change of SIR of the HV-PCB in this area would affect the sampling value of the divider resistor.

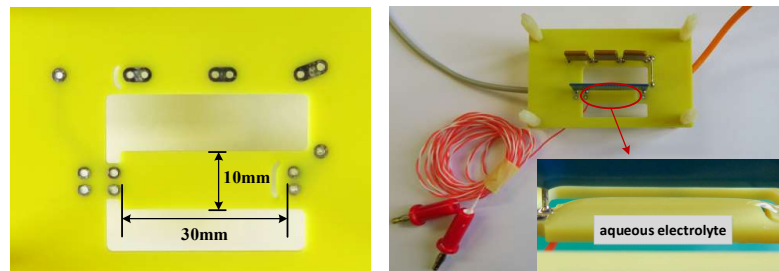


Figure 1. Test sample.

2.2. Test Sample Preparation

2.2.1. Divider Resistor

Divider resistors (divider ratio: 1000:1) were screened for temperature and humidity before use at 85 °C/95% RH, applying 7 kV DC continuously for 10 h. The sampling value of the divider resistor was 6.87 V, and the fluctuation did not exceed 0.01.

2.2.2. Preparation of the Test Boards

HV-PCBs were hand-welded with 63/37 solder and rosin-based RMA flux. The test boards were pre-dried at 85 °C for 2 h before welding. Solder joints were rounded to prevent tip discharge. PCBs were cleaned with absolute ethyl alcohol and a flux cleaning agent, respectively, after welding. According to IPC-TM-650, HV-PCBs were tested for ionic residues after cleaning. The test solution was a 3:1 mixture of 75 vol% of isopropanol (IPA) and 25 vol% of deionized water. The resistivity of the mixture was greater than 16 MΩ•cm, and the concentration of ionic residues obtained by the test were less than 1.56 μg/cm².

NaCl-contaminated samples were prepared as follows. NaCl solution was prepared with 18.2 MΩ•cm deionized water at concentrations of 0.05, 0.1, 0.2, 0.3, and 0.5 g/L. The ratio relationship between g/L and μg/cm² was 1:100 [5, 21], and the sampling area was 300 mm². A volume of 0.3 mL of NaCl solution was pipetted so that the concentration of ionic contamination in the sampling area was 5, 10, 20, 25, and 50 μg/cm². The extent of this pollution level was chosen considering the effects of contamination generated by the manufacturing process and soluble inorganic salts contained in indoor dust deposits in Beijing [30]. All samples were tested after 24 h at room temperature.

2.3. Testing Circuit

The test circuit is shown in Figure 2. In the system test, three samples of each pollution level were prepared in each group of tests, and three blank divider resistors were compared. These three divider resistors involved suspended welding to eliminate the interference of the printed board.

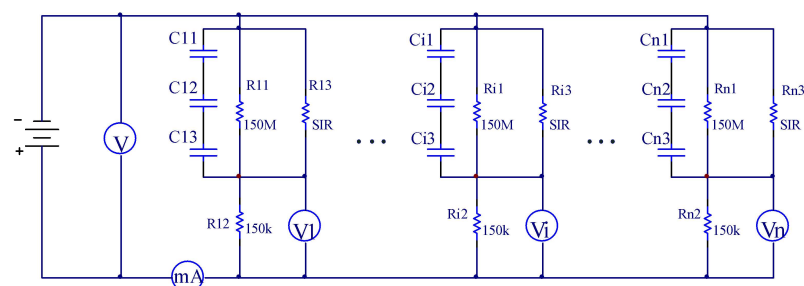


Figure 2. Test circuit.

SIR is the surface insulation resistance of the HV-PCB. Under clean and dry conditions, SIR is greater than 10¹² ohms, and does not affect the 150 M divider resistor.

2.4. Testing Condition

2.4.1. Damp Heat Test

Humidity and temperature are key factors affecting insulation performance. To find boundary conditions for degradation in insulation properties, humidity ranges from 35% to 95% were tested at intervals of 5 points. The high-temperature boundary was set at 85 °C, which was the highest environmental condition experienced by the product. Four temperature points of 30, 45, 65, and 85 °C were selected, which were the typical test temperatures of the product. The test was carried out at constant temperature with humidity gradually increasing from 35% to 95%. Each temperature and humidity point was maintained for 24 h before the test. A constant temperature point used with a total of four groups of tests. The test voltages were 4, 7, and 10 kV, corresponding to the three voltage levels of the product. The sampling value of the divider resistor was recorded from initial to stable during the test. If the sampling value has a very large jump, it indicates that there is a surface discharge on HV-PCB. In this case, the discharge process was filmed with a camera. The high-voltage was kept for 5 min and then was turned off. The test of the discharge type sample was ended when it returned to room temperature. The discharge state was observed with a microscope. SEM was used to observe surface topography. The hydrophilicity of the PCB after discharge was tested using a contact angle tester. The experiment was repeated three times and the average value was calculated.

2.4.2. Alternating Damp Heat Test

If the product is operated under conditions of temperature changes, the risk of condensation will increase. So, if condensation occurs on the surface of clean (ionic contamination concentration is less than $1.56 \mu\text{g}/\text{cm}^2$) product under extreme environmental changes, the insulation performance will change. To find out how this changes, we simulated the condensation of water that the product might experience under extreme environmental changes and carried out 40 cycle experiments on uncontaminated samples under rapid alternating damp heat conditions (referring to MIL-STD-202G temperature cycling conditions, while rapid temperature variation was used for temperature change rate). The test was performed on cycles 3, 14, 26, and 37, at temperature of 65 °C and humidity of 95% RH. The test voltages were 4, 7, and 10 kV, and the initial to final stable values were recorded. Figure 3 shows the test profile.

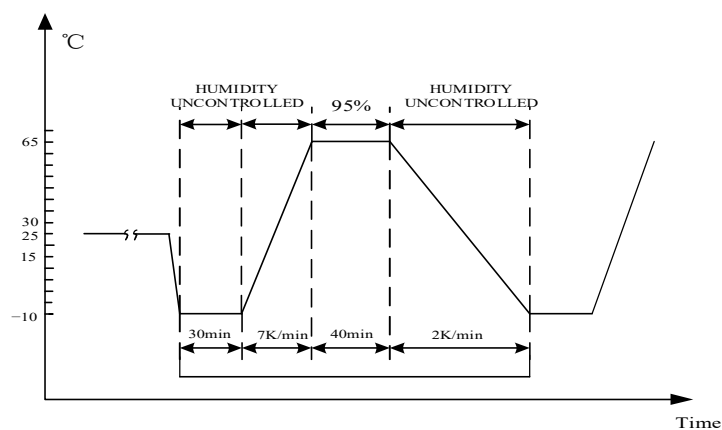


Figure 3. Test profile of alternating damp heat test.

2.5. Testing Platform

Figure 4 shows the test platform. Table 1 shows the information and functions of all the equipment in Figure 4.

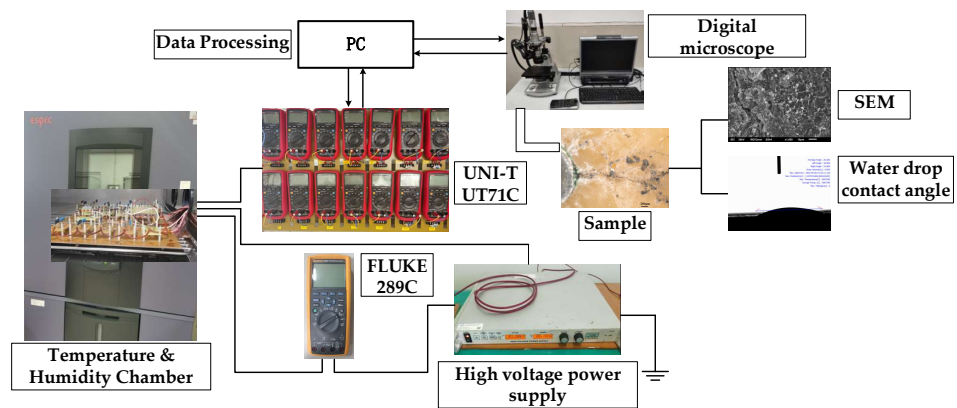


Figure 4. Test platform.

Table 1. Equipment list.

Device Name	Device Model	Function
Temperature and Humidity Chamber	Espec-GPS-5	Provides test conditions
DC high-voltage power supply	Iseg Hpn-300-106	Provides the voltage required for the test
Ammeter	FLUKE 289C	Detects the current in the test circuit
Multimeter	UNI-T UT71C	Tests the sampling value
Digital microscope	KEYENCE VHX-5000	Observes the appearance of the samples
SEM	JEOL JSM ■ 6510	Observes the microscopic morphology of the samples
Water drop angle tester	SEO Phoenix300	Tests the contact angle on the surface of the samples

3. Results

3.1. Boundaries of Deterioration of Insulation Properties

The test results show that there were two forms of deterioration of the insulation performance of HV-PCBs under thermal and moisture stress: decrease of SIR and surface discharge. Tables 2 and 3 show the starting points of the two forms of deterioration.

Table 2. Starting points of change in SIR.

Sample	Temperature (°C)	Relative Humidity (%)	Voltage (kV)
5 $\mu\text{g}/\text{cm}^2$	30	75	4
10 $\mu\text{g}/\text{cm}^2$	30	75	4
20 $\mu\text{g}/\text{cm}^2$	30	75	4
30 $\mu\text{g}/\text{cm}^2$	30	75	4
50 $\mu\text{g}/\text{cm}^2$	30	75	4
Uncontaminated	85	90	4

Table 3. Starting points of surface discharge.

Sample	Temperature (°C)	Relative Humidity (%)	Voltage(kV)
5 $\mu\text{g}/\text{cm}^2$	/*	/*	/*
10 $\mu\text{g}/\text{cm}^2$	85	95	10
20 $\mu\text{g}/\text{cm}^2$	85	95	10
30 $\mu\text{g}/\text{cm}^2$	85	90	7
30 $\mu\text{g}/\text{cm}^2$	65	95	7
50 $\mu\text{g}/\text{cm}^2$	85	85	7
50 $\mu\text{g}/\text{cm}^2$	65	90	7
50 $\mu\text{g}/\text{cm}^2$	45	95	7
Uncontaminated	/*	/*	/*

* Indicates that no surface discharge occurred under all conditions of the test.

Samples with different ionic contamination concentrations had deteriorated insulation properties under different temperature and humidity conditions. For ionic contaminated samples, the sampling value changed at 4 kV, 30 °C/75% RH. It should be noted that the sampling value of uncontaminated products also deviated at 85 °C/90% RH with a change value within 0.03, and when it rose to 85 °C at 95% RH, the change value increased to 0.1 at most. The starting point of the surface discharge showed the relationship with temperature, humidity, applied voltage, and ionic contaminant concentration. For example, 50 $\mu\text{g}/\text{cm}^2$ discharged at 7 kV and 45 °C/95% RH, while 20 $\mu\text{g}/\text{cm}^2$ discharged at 85 °C/95% RH and 10 kV.

Figure 5 shows products with a voltage level of 10 kV as an example to draw the insulation deterioration boundary diagram of products with different ionic contamination concentrations, i.e., the boundary where the sampling value of the divider resistor changes and the surface discharge of the HV-PCB occurs. The starting point of the change in the sampling value of the divider resistor means that the performance parameters of the product have shifted, suggesting initial failure. The starting point of surface discharge means that leakage occurs in the sampling area of the product, and the instantaneous short circuit may cause the breakdown of some components of the product, resulting in irreversible failure. The boundary diagram can be used to predict the insulation performance of products with different degrees of contamination under certain temperature and humidity conditions. Three hypothetical points are selected in Figure 6. Assuming that the ionic contamination concentration is 1.56 $\mu\text{g}/\text{cm}^2$, the deterioration of SIR will occur at 30 °C/95% RH. Similarly, when the ionic contamination concentration is 15.6 $\mu\text{g}/\text{cm}^2$, the deterioration of SIR will occur at 30 °C/75% RH. At an ionic contamination concentration of 32 $\mu\text{g}/\text{cm}^2$, the surface discharge will occur at 85 °C/92% RH.

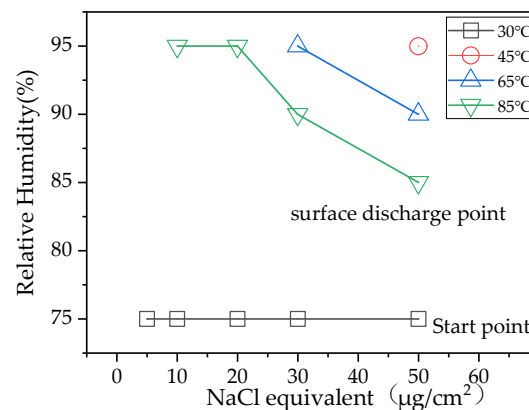


Figure 5. Boundary of insulation deterioration.

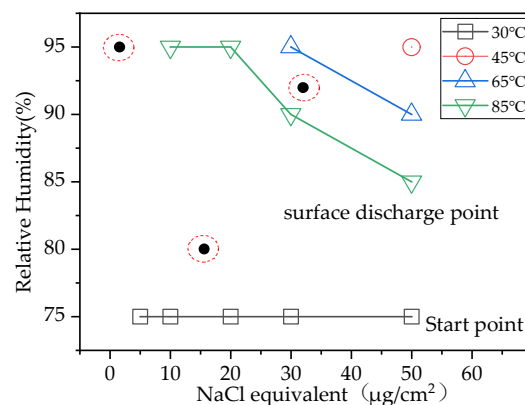


Figure 6. Prediction of insulation deterioration.

3.2. Effect of Humidity and Ionic Contamination

The presence of electrolyte and bias is considered necessary for a reduction in SIR of a PCB. When there is electrolyte on the surface of the PCB, the SIR of the PCB is recorded as $R_{humidity}$, which can be calculated by the circuit diagram in Figure 7 and the following calculation methods.

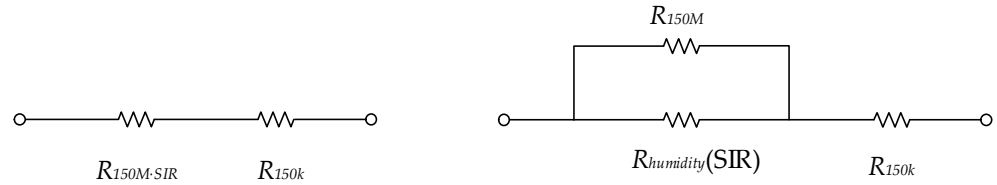


Figure 7. Circuit schematic diagram.

Calculation formula:

$$R_{150M \cdot SIR} = \frac{R_{150M} \cdot R_{humidity}}{R_{150M} + R_{humidity}} \tag{1}$$

$$R_{150k} = \frac{U_{150k}}{I} \tag{2}$$

$$R_{150M \cdot SIR} = \frac{U - U_{150k}}{I} \tag{3}$$

$$R_{humidity} = \frac{\frac{U - U_{150k}}{U_{150k}} \cdot R_{150k} \cdot R_{150M}}{R_{150M} - \frac{U - U_{150k}}{U_{150k}} \cdot R_{150k}} \tag{4}$$

where R_{150M} is the 150 MΩ divider resistor value, $R_{humidity}$ is SIR of PCB, R_{150k} is the 150 KΩ divider resistor value, $R_{150M \cdot SIR}$ is the parallel resistance of R_{150M} and $R_{humidity}$, U is the total voltage applied, U_{150k} is sampling value of divider resistor.

Figure 8 shows the variation of sample sampling values and SIR with different ionic concentrations at different relative humidity levels. When the sampling value is unchanged, it indicates that SIR has no effect on the divider resistor. An SIR in parallel on the 150M resistor has little effect on the resistance after paralleling, and then SIR is not drawn in the figure.

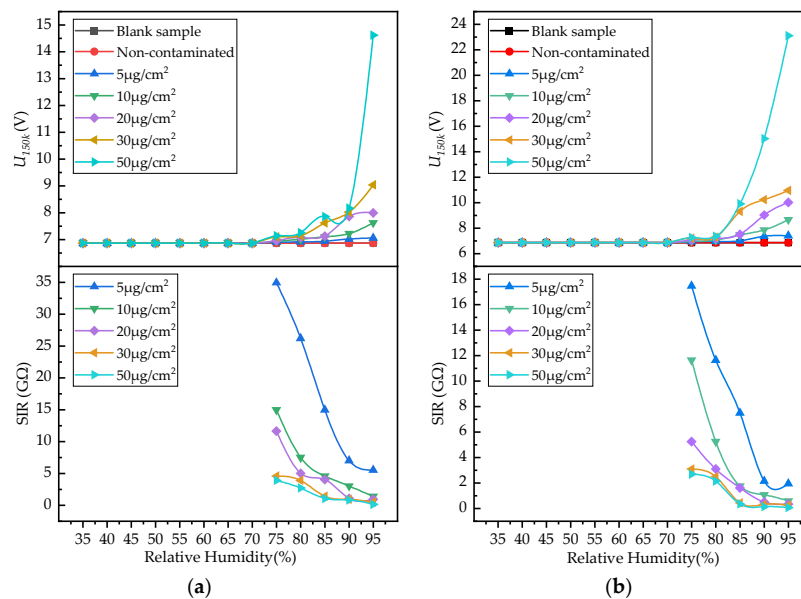


Figure 8. Cont.

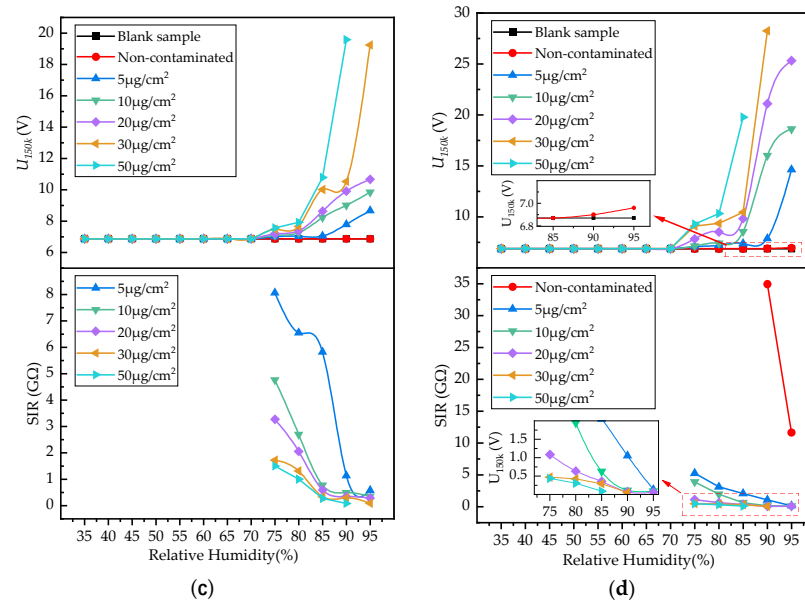


Figure 8. Variation law of sampling value of 7 kV at constant temperature and different humidities. (a) Temperature of 30 °C; (b) Temperature of 45 °C; (c) Temperature of 65 °C; (d) Temperature of 85 °C.

As shown in Figure 8, the critical humidity point of the insulation performance of HV-PCB begins to change under different temperature conditions at 75% RH. When the relative humidity is less than 75% RH, the sampling value of the divider resistor with different contamination concentrations does not change even if the temperature increases. Below a certain humidity, the influence of temperature on insulation performance can be ignored. When the relative humidity reaches 75% RH, the sampling value changes, which is related to temperature and concentration of ionic contamination. However, even for non-contaminated samples, the sampling value begins to increase at 85 °C/90% RH. At the same temperature, with the increase of the concentration of ionic contamination, greater variation of sampling values results in a smaller SIR of PCB.

3.3. Effect of Temperature and Ionic Contamination

Figure 9 shows the sampling values for different ionic contamination concentrations at different temperatures at relative humidities of 75% and 85%. The sampling values at different humidities show the same trend with temperature. The greater the change in the sampling value as the temperature increases leads to a smaller surface insulation resistance (SIR).

Similarly, the boundary point of the discharge is also related to temperature. For example, at a relative humidity of 95%, a sample of 50 $\mu\text{g}/\text{cm}^2$ discharges at 45 °C, but at 85 °C, a discharge also occurs at 10 $\mu\text{g}/\text{cm}^2$. This suggests that the applied voltage of the discharge is different. Figure 10 shows the effect of temperature on discharge boundaries.

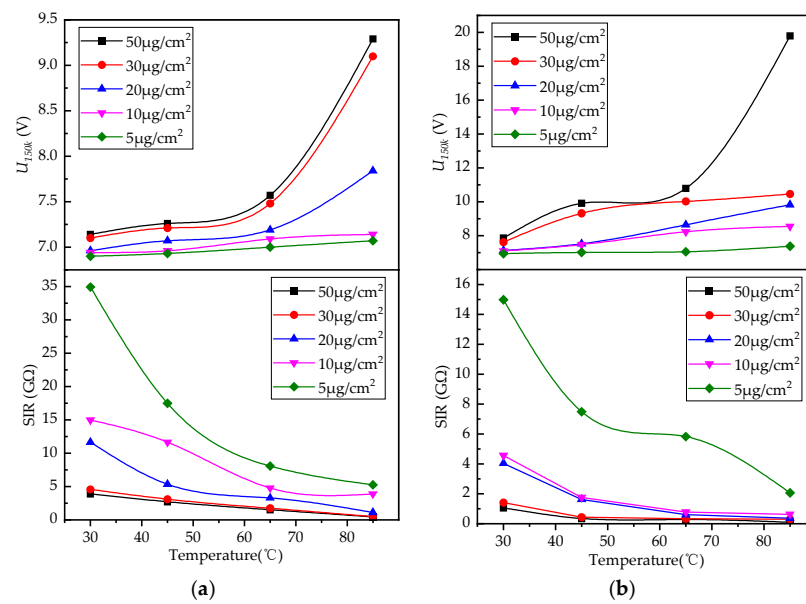


Figure 9. The influence of temperature on sampling value and SIR under different humidities; (a) relative humidity 75%; (b) relative humidity 85%.

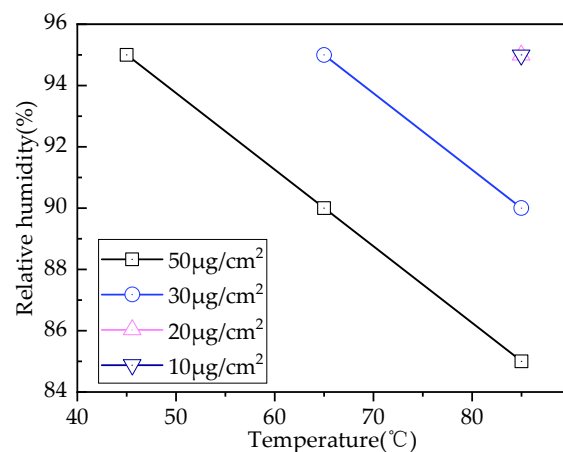


Figure 10. Effect of temperature on discharge boundary.

3.4. Surface Discharge of HV-PCB

Figure 11 shows a typical discharge phenomenon captured by camera. The discharge has an obvious spark and discharging path.



Figure 11. Discharge phenomenon.

We investigated the discharge characteristics of different morphology under two different ionic contamination concentrations. Figure 12 shows magnified microscope images

of a sample with $50\mu\text{g}/\text{cm}^2$ discharged at 7 kV, $45\text{ }^\circ\text{C}/95\%$ RH. Figure 13 shows the corresponding SEM images. Figure 14 shows magnified microscope images of a sample with $20\mu\text{g}/\text{cm}^2$ discharged at 10 kV, $85\text{ }^\circ\text{C}/95\%$ RH. Figure 15 shows the corresponding SEM images.

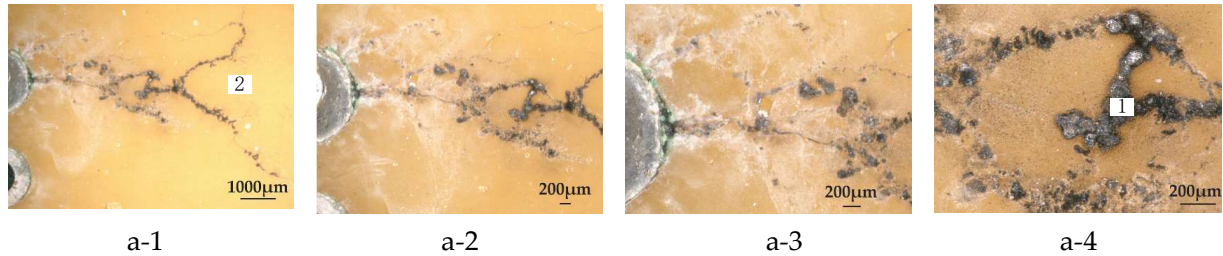


Figure 12. Discharge diagram of sample with $50\mu\text{g}/\text{cm}^2$ at 7 kV, $45\text{ }^\circ\text{C}/95\%$ RH. ((a-1)–(a-4)) are magnifications of 20 \times , 30 \times , 50 \times and 100 \times respectively.

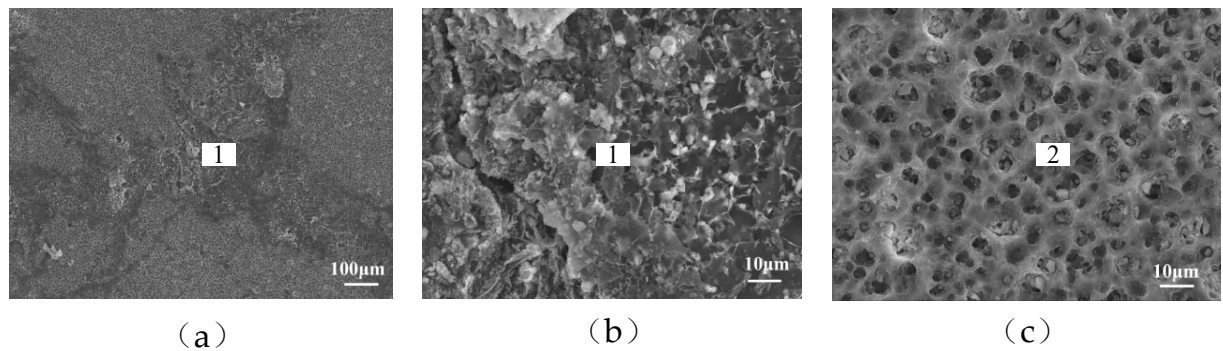


Figure 13. SEM images corresponding to the discharge sample in Figure 12. Numbers 1, 2 can be, respectively, found in Figure 12. (a) is magnifications of 100 \times , (b,c) are magnifications of 1000 \times , respectively.

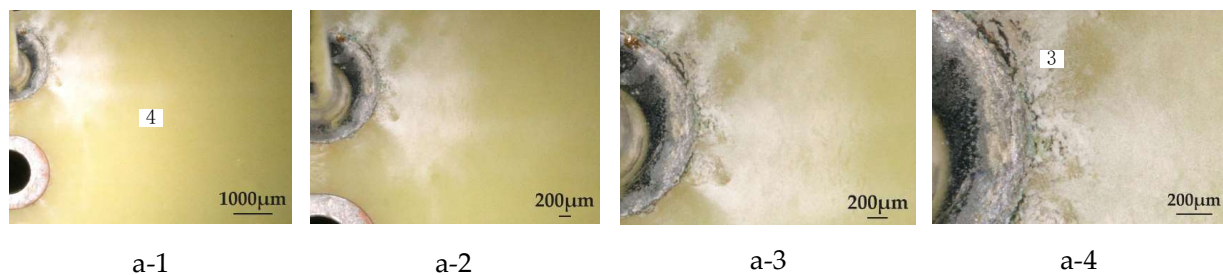


Figure 14. Discharge diagram of sample with $20\mu\text{g}/\text{cm}^2$ at 10 kV, $85\text{ }^\circ\text{C}/95\%$ RH. ((a-1)–(a-4)) are magnifications of 20 \times , 30 \times , 50 \times and 100 \times , respectively.

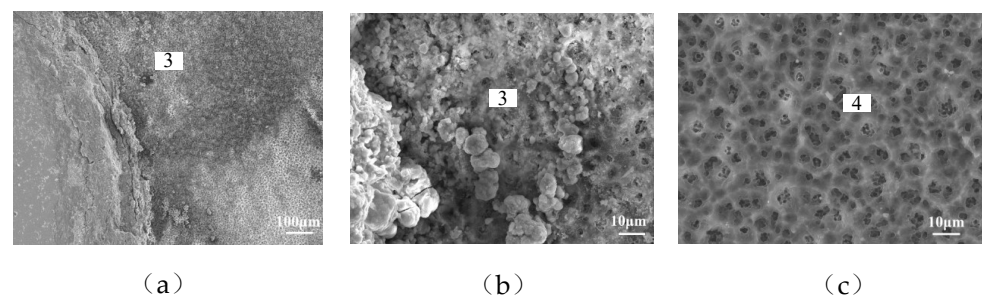


Figure 15. SEM images corresponding to the discharge sample in Figure 14. Numbers 3, 4 can be found in Figure 14. (a) is magnifications of 100 \times , (b,c) are magnifications of 1000 \times , respectively.

Figures 12 and 14 that show certain differences in the morphology of discharge with different concentrations. At an ionic concentration of $50 \mu\text{g}/\text{cm}^2$, the discharge showed a long dendritic shape with severe ablative traces on the surface. However, when the ionic concentration was $20 \mu\text{g}/\text{cm}^2$, the discharge traces were concentrated on the edge of the solder joint, showing a radial shape. The morphologies of the discharge regions and non-discharge regions with different concentrations were observed by SEM, and the non-discharge regions showed the same morphological characteristics. The morphology of the discharge region changed, showing different ablative morphology.

3.5. Effect of Condensation on Uncontaminated Samples

Figure 16 shows the sampling values of uncontaminated samples under the applied voltage of 7 kV at the 3rd, 14th, 26th, and 37th cycles of the rapid alternating damp-heat test. At each cycle test point, it could be observed through the window of the temperature and humidity test chamber that there were dense water droplets on the surface of PCBs, representing significant condensation. Compared with the maximum variation of the sampling value under constant temperature and humidity, the variation of the sampling value under condensing water condition was greater than 0.1. The initial sampling value for the third cycle was 7.06 V, which fluctuated by 0.19 compared to the original value of 6.87 V. The initial sampling value for the 37th cycle was 7.31 V, which fluctuated by 0.44. As the experiment progressed, the initial sampling value gradually increased. However, the sampling value tended to stabilise quickly, and the stable value was still larger than the initial value.

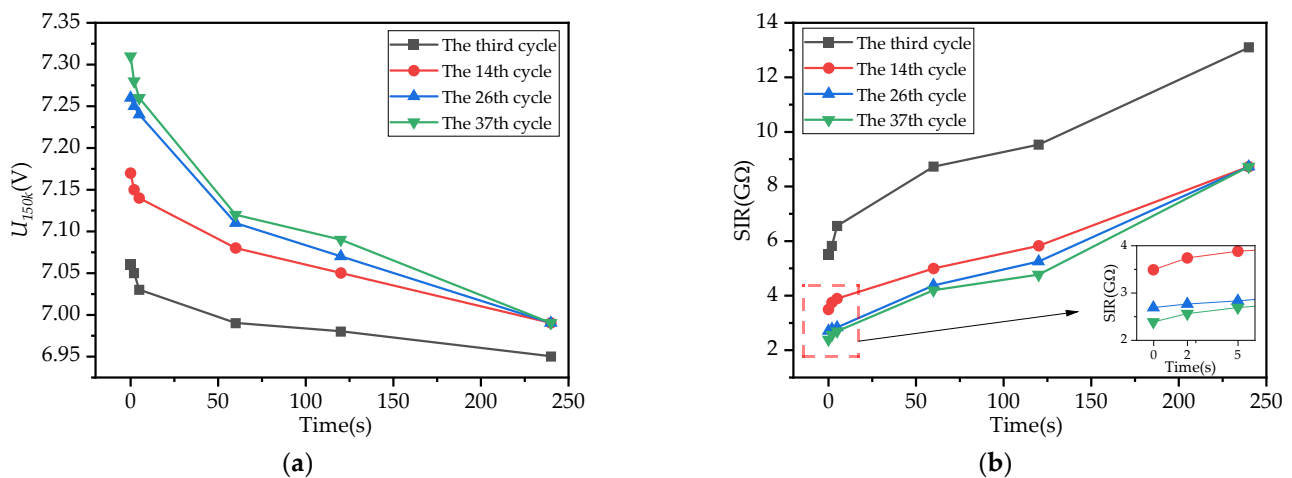


Figure 16. Change of sampling value during rapid alternating damp-heat test. (a) Change in sampling value, and (b) change in SIR.

3.6. Encapsulation Protection

The most common protection method for EPC is encapsulation. However, this process may introduce reliability risks associated with encapsulation, such as bubbles, interface contamination or delamination, and deterioration of potting materials in the space environment. After overcoming these difficulties, we obtained an effective potting solution. We only discuss the results of potting, and the detailed potting scheme and process are not discussed. Potting was carried out on the uncontaminated sample surface. Figure 17 shows the potting sample. According to the requirements of MIL-STD-202 and 2.4.2, humidity and temperature-related tests were carried out. The test requirements and applied voltage values are shown in Table 4. The test voltages were 4, 7, and 10 kV. Figure 18 shows that the sampling values after encapsulation were stable and unchanged. For unencapsulated samples, even if the surface was contamination-free, the sampling values increased by 0.03 at $85^\circ\text{C}/90\% \text{RH}$ and by 0.44 under alternating hot and humid conditions. Table 5 shows the comparison of sampling values for encapsulated and unencapsulated samples.

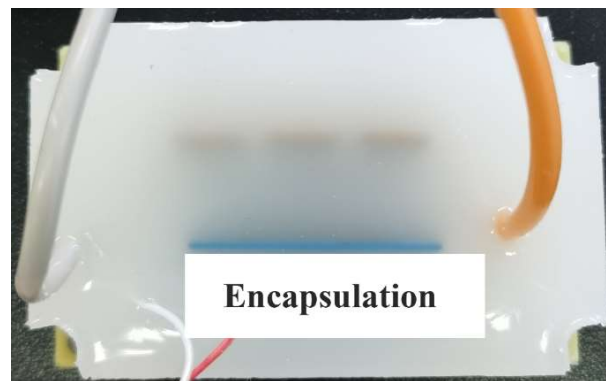


Figure 17. Potting sample.

Table 4. Test condition.

TEST	Test Project	Test Condition	Voltage (kV)
TEST-1	Humidity (steady State)	MIL-STD-202 103-A	4, 7, and 10
TEST-2	Moisture Resistance	MIL-STD-202 106	4, 7, and 10
TEST-3	Thermal shock	MIL-STD-202 107-B-1	4, 7, and 10
TEST-4	Alternating hot and humid	2.4.2	4, 7, and 10

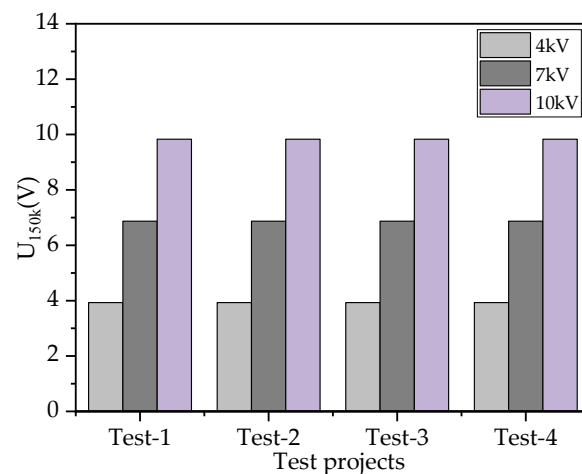


Figure 18. Sampling values after potting validation test.

Table 5. Comparison of sampling values for encapsulated and unencapsulated samples.

Sample	Minimum Deviation from the Sampling Value	Maximum Deviation of the Sampling Value
encapsulated samples	0	0
unencapsulated samples (non-contamination)	0.03 ¹	0.44

¹ A deviation of more than 0.01 in the sampling value will cause telemetry abnormality of TWTA.

4. Discussion

4.1. Analysis of the Influence of Temperature and Humidity on SIR

When ionic contaminants occur on the surface of the product, hydrophilic ionic contamination absorbs water in the humid environment and the solution changes from a crystalline solution to a saturated solution, (deliquescence) [31,32]. When the relative humidity reaches the critical relative humidity (CRH) of the contaminated salt, deliquescence of the contaminated salt occurs. NaCl is not only hydrophilic but also a strong electrolyte.

According to Kohlrausch's law [20], it is completely dissociated into Na^+ and Cl^- in water. In the absence of an electric field, ions diffuse along the surface of the PCB. After a long enough diffusion time (several hours), the ions will be uniformly distributed on the surface of the PCB, resulting in a small and essentially isotropic surface impedance. However, under the action of an applied electric field, ions change from random diffusion motion to movement in the direction of the power line, which is called ion migration, as shown in Figure 19. After ion migration, the positive ions gradually accumulate at the negative extreme of the electric field and the negative ions gradually accumulate at the positive extreme of the electric field. Humidity and temperature are the main factors affecting ion migration.

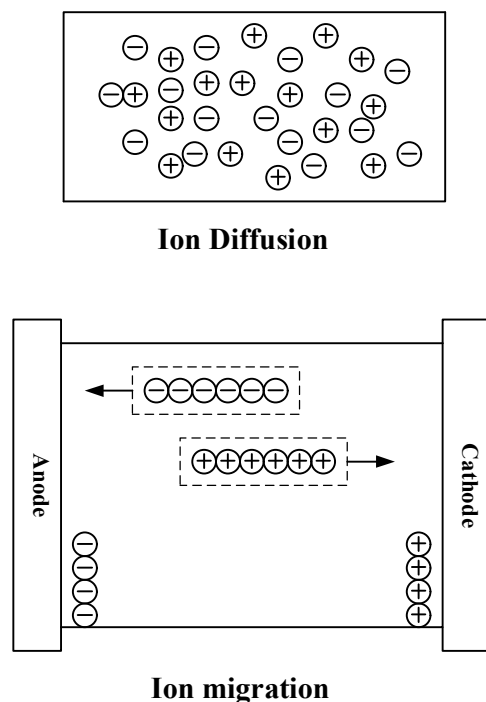


Figure 19. Diffusion and migration of ions.

The results show that the sampling values of all products did not change below 70% RH, and the change occurred at $\text{RH} \geq 75\%$ RH. With an increase in temperature, the relative humidity point where the change occurred did not decrease significantly. This is because the CRH of NaCl at 20~40 °C is 75% RH. In addition, as the ionic bond breakage does not generate heat during the dissolution of sodium chloride, solubility does not increase with the increase in temperature, which means that the increase in temperature has little influence on the relative humidity of NaCl. The influence of temperature on SIR is reflected in the degree of deterioration. Under the same relative humidity conditions, the more severe deterioration occurs as the temperature increases, which is reflected in the product, and the greater the deviation of the telemetry parameters from the normal value.

Temperature and humidity have a synergistic effect on SIR. Humidity is the main factor, providing the necessary moisture for the formation of the electrolyte. The influence of temperature on electronic products has two factors. On the one hand, the increase in temperature increases the content of water vapor in the air. On the other hand, the increase in temperature reduces the viscosity of the saturated solution and accelerates ion mobility [33].

In general, the variation of insulation performance of HV-PCB under temperature and humidity stress has similar and different effects on low-voltage PCBs. When the fault form of the high-voltage printed board is only manifested as a decrease in SIR, its main influencing factors and change trend are the same as those of a low voltage printed

board. The difference is that surface discharge occurs in the high-voltage PCB under certain conditions.

4.2. Analysis of Surface Discharge

Surface discharge generally occurs in a gas (or liquid) with a tangential electric field on the surface of a solid dielectric. Surface discharge occurs only when the applied voltage reaches a certain value, i.e., the surface discharge voltage. The surface discharge voltage is closely related to the surface condition of the solid (such as contamination, moisture absorption, and surface roughness) [34,35]. When the relative humidity of the environment is higher than the critical relative humidity of the soluble salt on the insulation surface, the pollutants dissolve due to the adsorption of moisture, and the electrolyte is ionized. The movement of ions in the electric field is affected by the electric field force, which is linearly related to the electric field strength. The electric field strength affects the movement time of ions in the electrolyte. The strength of the electric field depends on voltage, geometric parameters (such as distance and shape), dielectric properties, and space charge. For parallel planes, when space charges and their synergistic effects are not considered [3],

$$E_{mean} = \frac{U}{d} \quad (5)$$

where E_{mean} is the average electric field, U is the applied voltage, and d is the gap length.

At a constant d , the applied voltage promotes the movement of ions. At the same time, temperature also plays a role in promoting the movement of ions.

Under the action of a surface electric field and ionic contamination, a large leakage current flows along the surface of the PCB [34,35]. The thermal effect of the leakage current causes electrolyte in some micro-regions to begin to evaporate, forming local dry areas. The formation of a local drying zone causes a sudden interruption of the electric current, followed by a spark discharge and the release of more heat. Multiple discharges degrade the surface of PCB, forming a carbonization channel, that is, an electric trace [29]. With the development of discharge time, the carbonization channel formed through the whole electrode, and the insulation performance of PCB surface, will fail. Figure 20 shows the carbonization channel through a PCB with an ionic contamination concentration of $100 \mu\text{g}/\text{cm}^2$ within 10 min under a 7 kV applied voltage and 85 °C/85% RH.



Figure 20. Carbonization channel through a PCB with an ionic contamination concentration of $100 \mu\text{g}/\text{cm}^2$ within 10 min under a 7 kV applied voltage and 85 °C/85% RH.

In addition, the hydrophilicity of the material surface also changes during repeated surface discharges. This can be confirmed by an infiltration test of the sample surface after the test. The water contact angle indicates wetting between the water and PCB [36]. Figure 21 shows the contact angle of an uncontaminated sample, and 50 and $20 \mu\text{g}/\text{cm}^2$ samples. Figure 22 shows the change in the curve of the contact angle on the surface of different contaminated samples. The higher the concentration of ionic contaminants, the smaller the droplet angle. This is because, under the synergistic effect of electrical and thermal stress in the process of discharge, the organic polymer chains on the surface of

the PCB decompose and break off, resulting in electrical erosion changes. The number of surface hydrophobic groups gradually decreases, and the roughness gradually increases, which further reduces the hydrophobicity of the PCB.

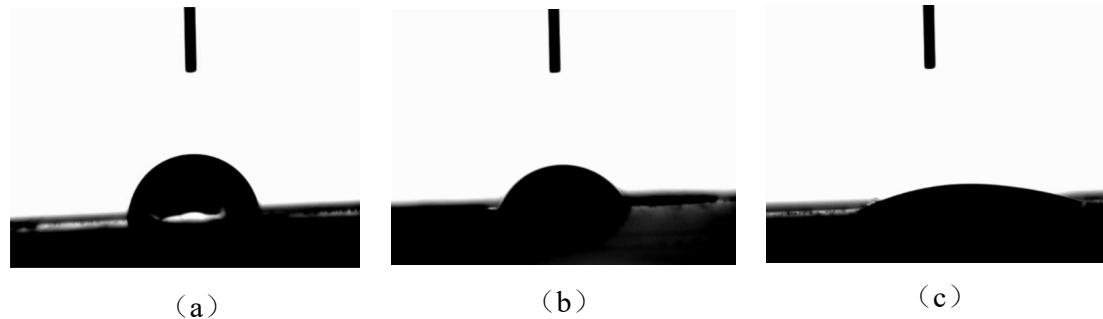


Figure 21. Contact Angle of an uncontaminated sample, and 20 $\mu\text{g}/\text{cm}^2$ and 50 $\mu\text{g}/\text{cm}^2$ samples.

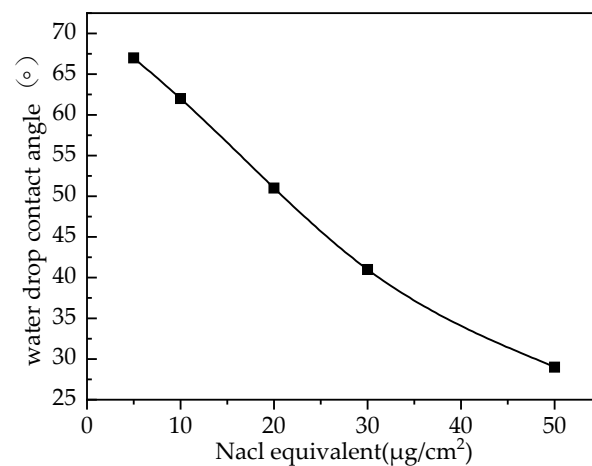


Figure 22. Contact angle at different pollution concentrations.

4.3. Analysis of Clean Surface

Surface contaminants, especially ionic contaminants, may have a significant impact on the entire ion migration process. However, ionic contaminants may not be essential for migration compared to the presence of water. In the test, we found that the sampling value of the uncontaminated sample changed at 85 $^\circ\text{C}/90\%$ RH and 95% RH. Moreover, in the rapid alternating damp heat test, the change value was greatly increased. This indicates that under these conditions, ion migration occurs on the surface of PCB.

On the one hand, pure water has a fairly low conductivity through the proton jumping mechanism [37], as shown in Equation (6):



On the other hand, water would further exacerbate conductivity if it absorbs from the atmosphere gases with which it forms compounds such as CO_2 [38].



The conductivity of water is related to the thickness of the water film [39]. In the rapid alternating damp heat test, there were condensed water droplets (bulk water) on the surface of the PCB, and the thickness of the water layer was much thicker than the thickness of the water film adsorbed on the PCB under the condition of constant temperature and humidity. This is why the sampling value changed much more in the rapid alternating test than under constant temperature and humidity conditions.

It can be seen defining the uncontaminated sample as having ionic contamination at a concentration of less than $1.56 \mu\text{g}/\text{cm}^2$ is not completely appropriate. The limit of $1.56 \mu\text{g}/\text{cm}^2$ was taken from IPC-J-STD-001H. How to identify the qualified cleaning manufacturing process, and how to carry out effective protection is still a direction for future research.

Encapsulation has proven to be an effective form of protection. Encapsulation reliability involves materials, design, process, and testing. Breakdown of the potting interface is the main failure mode of encapsulation [40]. An in-depth understanding of its breakdown mechanism, influencing factors and how to suppress them, requires further study

5. Conclusions

A typical EPC circuit was used to study the influence of ion contamination on insulation failure of HV printed boards using temperature and humidity bias tests. The starting temperature, humidity, and surface discharge boundary of the insulation of EPC were obtained. Our conclusions provide a reference for further strengthening the environmental protection requirements during the development of EPCs.

The insulation deterioration of EPC occurred when the relative humidity was 75% or above, and the degree of deterioration was related to temperature and NaCl concentration.

The uncontaminated samples (ionic contamination concentration was less than $1.56 \mu\text{g}/\text{cm}^2$) and had slight changes at $85^\circ\text{C}/90\text{ RH}$. Condensation from rapidly alternating damp heat exacerbated the change.

Pure NaCl was used as the equivalent contaminant, but the actual contaminants should be complexes of NaCl with small amounts of other soluble salts. Their critical relative humidities will be somewhat different from that of pure NaCl, resulting in some deviations in the initial failure point. The actual composition and characteristics of contaminants on the surface of high-voltage PCBs will be further studied to correct the deviation of the failure point.

Here, it is proposed to use encapsulation to protect the EPC, and the humidity and temperature-related tests were verified according to MIL-STD-202. However, it is worth noting that the problem of potting interface discharge still needs further attention.

Author Contributions: Conceptualization, C.H. and G.W.; methodology, C.H., G.W., Y.F. and B.Z.; validation, C.H., W.Z. and B.Z.; formal analysis, C.H.; investigation, C.H. and Y.F.; resources, C.H. and W.Z.; data curation, C.H. and W.Z.; writing—original draft preparation, C.H.; writing—review and editing, B.Z., G.W., Y.F., H.L. and K.Z.; visualization, W.Z.; supervision, C.H.; project administration, C.H.; funding acquisition, C.H. All authors have read and agreed to the published version of the manuscript.

Funding: This research received no external funding.

Data Availability Statement: Not applicable.

Conflicts of Interest: The authors declare no conflict of interest.

References

1. Li, Z.-C. The current status and developmental trends of space travelling wave tube amplifier. *Space Electron. Technol.* **2012**, *4*, 28–34.
2. Pequet, E.; Delporte, P.; Fayt, P.; Gak, M.; Canon, T. ESA qualified EPC for telecommunication satellites TWTA. In Proceedings of the Abstracts. International Vacuum Electronics Conference 2000 (Cat. No. 00EX392), Monterey, CA, USA, 2–4 May 2000; pp. 1–2.
3. Secretariat, E.C.S.S. *Space Engineering High-Voltage Engineering and Design Handbook*; ESA Special Publication: Noordwijk, The Netherlands, 2014; p. 133.
4. Tegehall, P.-E. Impact of humidity and contamination on surface insulation resistance and electrochemical migration. In *The ELFNET Book on Failure Mechanisms, Testing Methods, and Quality Issues of Lead-Free Solder Interconnects*; Springer: London, UK, 2011; pp. 227–253.
5. Verdingovas, V.; Jellesen, M.S.; Ambat, R. Impact of NaCl contamination and climatic conditions on the reliability of printed circuit board assemblies. *IEEE Trans. Device Mater. Reliab.* **2013**, *14*, 42–51. [[CrossRef](#)]
6. Hansen, K.S.; Jellesen, M.S.; Moller, P.; Westermann, P.J.S.; Ambat, R. Effect of solder flux residues on corrosion of electronics. In Proceedings of the 2009 Annual Reliability and Maintainability Symposium, Fort Worth, TX, USA, 26–29 January 2009; pp. 502–508.

7. Piotrowska, K.; Verdingovas, V.; Ambat, R. Humidity-related failures in electronics: Effect of binary mixtures of weak organic acid activators. *J. Mater. Sci. Mater. Electron.* **2018**, *29*, 17834–17852. [[CrossRef](#)]
8. Verdingovas, V.; Jellesen, M.S.; Ambat, R. Relative effect of solder flux chemistry on the humidity related failures in electronics. *Solder. Surf. Mt. Technol.* **2015**, *27*, 146–156. [[CrossRef](#)]
9. Song, B.; Azarian, M.H.; Pecht, M.G. Effect of temperature and relative humidity on the impedance degradation of dust-contaminated electronics. *J. Electrochem. Soc.* **2013**, *160*, C97. [[CrossRef](#)]
10. Zhou, Y.; Xie, Q. Effect of dust pollution on temperature characteristics of electrochemical migration. In Proceedings of the 2017 Prognostics and System Health Management Conference (PHM-Harbin), Harbin, China, 9–12 July 2017; pp. 1–6.
11. Song, B.; Azarian, M.H.; Pecht, M.G. Impact of dust on printed circuit assembly reliability. In Proceedings of the IPC APEX EXPO, San Diego, CA, USA; 2012; Volume 3, pp. 1643–1659.
12. Xie, C.; Tang, X.; Song, B.; Jin, J. Study on the Effect of Moisture Stress on Printed Circuit Board of Numerical Control System. In Proceedings of the 2012 Second International Conference on Instrumentation, Measurement, Computer, Communication and Control, Harbin, China, 8–10 December 2012; pp. 1661–1665.
13. Zhong, X.; Yu, S.; Chen, L.; Hu, J.; Zhang, Z. Test methods for electrochemical migration: A review. *J. Mater. Sci. Mater. Electron.* **2017**, *28*, 2279–2289. [[CrossRef](#)]
14. Medgyes, B.; Illés, B.; Harsányi, G. Electrochemical migration behaviour of Cu, Sn, Ag and Sn63/Pb37. *J. Mater. Sci. Mater. Electron.* **2012**, *23*, 551–556. [[CrossRef](#)]
15. Medgyes, B.; Illés, B.; Harsányi, G. Effect of water condensation on electrochemical migration in case of FR4 and polyimide substrates. *J. Mater. Sci. Mater. Electron.* **2013**, *24*, 2315–2321. [[CrossRef](#)]
16. Minzari, D.; Jellesen, M.S.; Moller, P.; Wahlberg, P.; Ambat, R. Electrochemical migration on electronic chip resistors in chloride environments. *IEEE Trans. Device Mater. Reliab.* **2009**, *9*, 392–402. [[CrossRef](#)]
17. Medgyes, B.; Zhong, X.; Harsányi, G. The effect of chloride ion concentration on electrochemical migration of copper. *J. Mater. Sci. Mater. Electron.* **2015**, *26*, 2010–2015. [[CrossRef](#)]
18. Tegehall, P.E.; Dunn, B.D. *Evaluation of Cleanliness Test Methods for Spacecraft PCB Assemblies*; ESA Publications: Auckland, New Zealand, 2006; Volume 275.
19. Verdingovas, V.; Jellesen, M.S.; Ambat, R. Solder flux residues and humidity-related failures in electronics: Relative effects of weak organic acids used in no-clean flux systems. *J. Electron. Mater.* **2015**, *44*, 1116–1127. [[CrossRef](#)]
20. Verdingovas, V.; Jellesen, M.S.; Ambat, R. Influence of sodium chloride and weak organic acids (flux residues) on electrochemical migration of tin on surface mount chip components. *Corros. Eng. Sci. Technol.* **2013**, *48*, 426–435. [[CrossRef](#)]
21. Tegehall, P.E.; Dunn, B.D. Influence of flux residues and conformal coatings on the surface resistance properties of spacecraft circuit boards. *ESA J.* **1992**, *16*, 255–273.
22. Hunt, C.; Zou, L. The impact of temperature and humidity conditions on surface insulation resistance values for various fluxes. *Solder. Surf. Mt. Technol.* **1999**, *11*, 36–43. [[CrossRef](#)]
23. Zhou, Y.-L.; Lan, D.-F. Effects of soluble salts in dust on insulation failure of printed circuit boards. *Trans. China Electrotech. Soc.* **2016**, *31*, 114–119.
24. Bahrebar, S.; Ambat, R. Investigation of critical factors effect to predict leakage current and time to failure due to ECM on PCB under humidity. *Microelectron. Reliab.* **2021**, *127*, 114418. [[CrossRef](#)]
25. Bahrebar, S.; Ambat, R. Time to Failure Prediction on a Printed Circuit Board Surface Under Humidity Using Probabilistic Analysis. *J. Electron. Mater.* **2022**, *51*, 4388–4406. [[CrossRef](#)]
26. Zhan, S.; Azarian, M.H.; Pecht, M.G. Surface insulation resistance of conformally coated printed circuit boards processed with no-clean flux. *IEEE Trans. Electron. Packag. Manuf.* **2006**, *29*, 217–223. [[CrossRef](#)]
27. Mancke, R. A moisture protection screening test for hybrid circuit encapsulants. *IEEE Trans. Compon. Hybrids Manuf. Technol.* **1981**, *4*, 492–498. [[CrossRef](#)]
28. Yi, P.; Dong, C.-F.; Xiao, K.; Wei, D. Current status and prospects of electrochemical migration research. *Sci. Technol. Rev.* **2018**, *36*, 64–73.
29. Du, B.-X.; Xu, H.; Li, Y.-P.; Li, Z.-L. Study on characteristics of tracking resistance of silicon rubber composite insulators with high thermal conductivity for UHVDC transmission lines. *High-Volt. Eng.* **2013**, *39*, 2910–2915.
30. Zhou, Y.-L.; Wang, P.; Ge, S.-C.; Li, F. Investigation on Dust Contamination of Aerospace Electrical Connector after Long-Term Storage. *Trans. China Electrotech. Soc.* **2014**, *29*, 269–276.
31. Conseil-Gudla, H.; Jellesen, M.S.; Ambat, R. Printed circuit board surface finish and effects of chloride contamination, electric field, and humidity on corrosion reliability. *J. Electron. Mater.* **2017**, *46*, 817–825. [[CrossRef](#)]
32. Harmon, C.W.; Grimm, R.L.; McIntire, T.M.; Peterson, M.D.; Njegic, B.; Angel, V.M.; Alshawa, A.; Underwood, J.S.; Tobias, D.J.; Gerber, R.B.; et al. Hygroscopic growth and deliquescence of NaCl nanoparticles mixed with surfactant SDS. *J. Phys. Chem. B* **2010**, *114*, 2435–2449. [[CrossRef](#)]
33. Korson, L.; Drost-Hansen, W.; Millero, F.J. Viscosity of water at various temperatures. *J. Phys. Chem.* **1969**, *73*, 34–39. [[CrossRef](#)]
34. Wang, J.-H.; Zhong, L.-S. *Handbook of Electrical Electronic Insulation Technology*; China Machine Press: Beijing, China, 2008.
35. Liang, X.-D. *High-Voltage Engineering*; Tsinghua University Press: Beijing, China, 2003.
36. Awakuni, Y.; Calderwood, J.H. Water vapour adsorption and surface conductivity in solids. *J. Phys. D Appl. Phys.* **1972**, *5*, 1038. [[CrossRef](#)]

37. Harsanyi, G. Irregular effect of chloride impurities on migration failure reliability: Contradictions or understandable? *Microelectron. Reliab.* **1999**, *39*, 1407–1411. [[CrossRef](#)]
38. Sbar, N.L.; Kozakiewicz, R.P. New acceleration factors for temperature, humidity, bias testing. In Proceedings of the 16th International Reliability Physics Symposium, San Diego, CA, USA, 18–20 April 1978; pp. 161–178.
39. Yan, B.D.; Meilink, S.; Warren, G.; Wynblatt, P. Water adsorption and surface conductivity measurements on alpha-alumina substrates. *IEEE Trans. Compon. Hybrids Manuf. Technol.* **1987**, *10*, 247–251.
40. Sato, M.; Kumada, A.; Hidaka, K.; Yamashiro, K.; Hayase, Y.; Takano, T. On the nature of surface discharges in silicone-gel: Prebreakdown discharges in cavities. In Proceedings of the 2014 IEEE Conference on Electrical Insulation and Dielectric Phenomena (CEIDP), Des Moines, IA, USA, 19–22 October 2014; pp. 19–22.